Hydrodynamics Investigations of Kaffir Lime Leaves Drying in a Swirling Solar Drying Chamber with Inclined Slotted Angle Air Distributor

Muhammad Amirul Azwan Azmi[1], Amir Abdul Razak[1,*], Muhammad Amir Syahiran Muhammad Tarminzi[1], Ahmad Fadzil Sharol[1], Ahmmad Shukrie Md Yudin[1], Zafri Azran Abdul Majid[2]

[1] Energy Sustainability Focus Group (ESFG), Faculty of Mechanical and Automotive Engineering Technology, Universiti Malaysia Pahang, Pekan, Pahang, Malaysia
[2] Kuliyyah of Allied Health Sciences, International Islamic University of Malaysia, Kuantan, Pahang, Malaysia

ARTICLE INFO

ABSTRACT

The present work aims to investigate the behavior of drying kaffir lime leaves in a swirling solar drying chamber (S-SDC) fitted with an inclined slotted angle air distributor. A distributor plated with inclined slotted angle was located at the air inlet at the bottom of the chamber. Experimental and numerical methods have been applied to analyze the efficiency of developed S-SDC assisted solar drying system based on the moisture content (MC), moisture content ratio (MR) and drying rate (DR) were examined. The experimental results showed that the S-SDC can reduce the moisture content of kaffir lime leaves more rapidly than a conventional solar drying chamber (CSDC). The S-SDC gave a higher DR and decreased drying time compared to that of C-SDC. The results also indicated that operation at higher air velocities resulted in a greater DR, especially at the beginning stage of the drying process. For the S-SDC, the reduced of MC, MR and DR at a high air velocity (v = 2.0 m/s) was better than at low air velocities (v = 0.5 and 1.0 m/s). Drying chamber efficiency is also observed at a higher air velocity of 2 m/s for both SSDC and CSDC. In addition, obtained experimental findings are in line with numerical results. The outcomes of this study present the potential of using the S-SDC compared to the C-SDC to be used in drying crops.

1. Introduction

In agricultural sector, the solar energy is used to dry crops since it is practical, can cut the cost of heat source since the heat can freely available and it do not harm the environment [1]. Solar heating system is built to improve the traditional drying method. Solar dryer, which uses the heating system can produce better quality products and it also can increase yield of the products since less waste are produced [2]. Rabha and Muthukumar [3] had stated that solar dryer is an efficient device that can be used to replace direct open sun drying. The main purpose of the drying process is to make sure that the products can be stored in a longer period by reducing the moisture content inside the product to the safe storage level [3]. However, this process consumes a lot of time and is energy

---

intensive. So, reducing the drying period and the energy demand is one of the main goal of a solar dryer by developing an efficient drying system [4]. Low moisture content can create a cost effective way by reducing the mass as well as the volume of the products which can help to minimize the packing, storage and transportation cost [5]. Efforts have been made to improve the efficiency of the solar drying system by analyzing the parameters namely the selection of materials for components in the system, loading and pre-treatments, drying temperature achieved in the drying chamber, the fluid velocity and relative humidity [6]. In open or natural sun drying, the crops are laid simply on the floor or mat in the full sunny days. As the crops being exposed directly to the sun, it gets contaminated from dirt and pest infestation and also lost by birds and beast. Researchers developed various type and method of drying chamber for solar dryer like cabinet, cylindrical, greenhouse etc. Such drying chamber are using around the world for drying of agricultural and non-agricultural products to keep the product hygiene and good qualities [5-8].

Solar drying chamber are installed in the drying system to heat the material and the place where the material to be dried is placed. The variation of targeted temperature can be achieved depending upon the industrial purposes with consistent air temperature inlet. Drying with an optimum temperature can ensure higher product quality since it will not harm the nutritional value of the products like vegetables and fruits. It is important for agricultural product preservation and is commercially applied for drying process and engineering application [9]. Solar drying chamber is currently used for drying processes in several industries and have been studied by many investigators. Etim *et al.,* [4] examined the influence of hot inlet air temperatures on the solar dryer performance and drying characteristics of drying banana. Mehta *et al.,* [5] examined the drying behaviour of fish-drying in solar dryer at various air temperatures (60–80°C). Their results showed that the drying air temperatures in the range of 60–65 °C attained inside the drying chamber was adequate to dry the fish. Additionally, the quality of the products dried in the drying chamber were comparable to those of sun dried materials. It was recommended that raw materials with high moisture contents should be dried at 60 °C to attain a high drying rate and reasonable drying time. Gulcimen *et al.,* [6] studied the drying moisture content within sweet basil in solar dryer at different mass flow rates of 0.012 kg/s, 0.026 kg/s, and 0.033 kg/s. They reported that the best drying efficiency is depending on mass flow rates at 420 min for 0.033 kg/s.

Recently, development of a modified solar drying chamber for enhancing the drying rate of crops was reported [7-10]. Tarminzi *et al.,* [7] conducted experiments to investigate the drying behaviors of the kaffir lime leaves crops in a cylindrical solar drying chamber with an arrangement's efficiency was evaluated based on the drying chamber's thermal delivery from the collectors, thermal gains and drying efficiencies, including air velocity effect and pressure drop. Their result shows that average air temperature in the drying chamber for was 49.9C and the maximum overall drying system efficiency is 31.82%. Islam *et al.,* [8] used a cabinet type solar dryer for drying fruits. They found that their dryer reduced total moisture removal rate of natural draft chamber was 58.9% which was highest among the three drying chamber and 33.3% for the attic space type chamber which was lowest among them. The use of the different fruits has different rate of moisture loss percentage which is for pineapple as it contains maximum amount of water among these four items but for guava as it contains less amount of water. Khanchi and Birrell [9] evaluate the effect of drying rate crops during field drying at various wind speed and was found to be dependent on solar radiation and influence of temperature in the chamber to dry the crops. Çakmak and Yıldız [10] developed a swirling flow dryer using hydrodynamics investigation with CFD simulation to increase the performance of pepper drying in a swirling fluidized bed dryer a solar collector that was used to heat air and compared its drying period with an open-air dryer operated under natural conditions. They reported that a decrease in the drying velocity resulted in increased drying time.

Based on the conducted literature review, there are fewer studies signifies the importance of the difference between the configuration and design of solar drying chamber. Most of the previous papers focused on studying and improving the overall solar drying systems' performance without emphasizing on the factors that cause the influence of drying chamber for drying products in order to achieve desired optimum temperature and air flow rate. The primary purpose of this study is to determine the best performance for the solar drying chamber and the results will be crucial for the researcher or practitioner to decide which configuration they should adapt in enhancing heat and mass transfer rates for solar dryer system. Therefore, in this paper, the effect of using SSDC that inserted of inclined slotted angle air distributor as can be seen in Figure 1 and Figure 2 are investigated. A conventional solar drying chamber (CSDC) without an inclined slotted angle air distributor plate was also tested for an assessment. Thermal performance for both drying chambers was observed and compared under several operating parameters. Finally, both system performances were evaluated based on the drying process of kaffir lime leaves in order to determine the most efficient drying chamber configuration for the particular drying process. Drying performance is strongly dependent on the drying methods and conditions used [11-16].
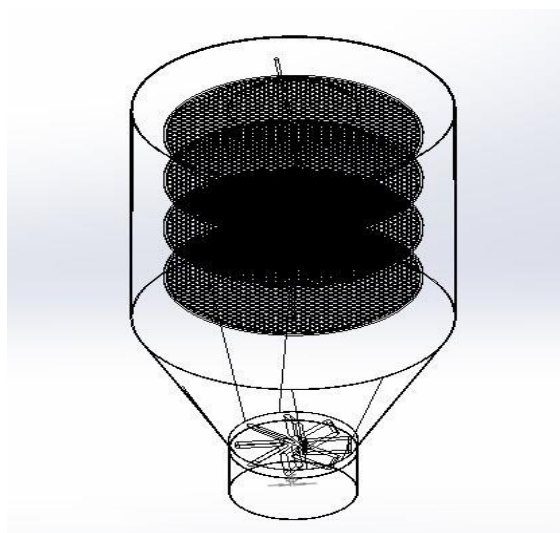
Fig. 1. Details of the swirling solar drying chamber with inclined slotted angle air distributor installed at the bottom of the chamber
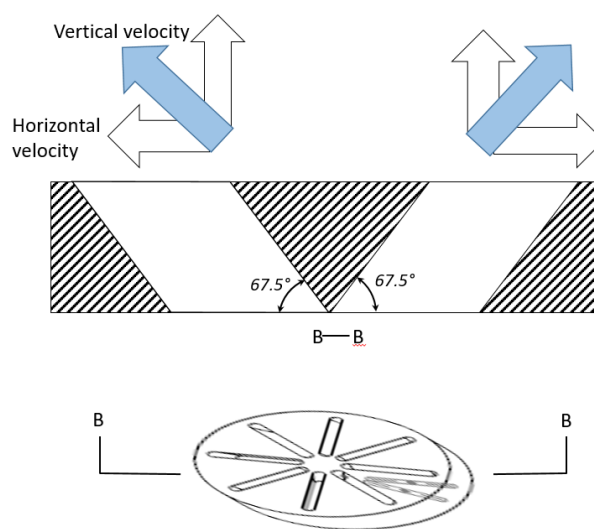
Fig. 2. Details of the inclined slotted angle air distributor

2. Methodology
2.1 Simulation Setup

One of the main objectives of the present study is to develop a 3D model for SSDC and CSDC as well as the inclined slotted angle air distributor using CFD method for evaluating thermal energy and temperature distribution of the drying chamber. Besides the theoretical calculations, simulation analysis is useful in providing better comparison between obtained results, which has been performed in this study. Simulation study of this work has been performed using Ansys Fluent software as a CFD program to examine behavior of solar drying chamber. In this study, two various configurations of solar drying chamber have been designed and manufactured to enhance the performance of solar drying system. In the first step, SSDC and CSDC have been designed and simulated. The main aim of this simulation is to compare the effectiveness of air flow rate pattern and temperature distribution by analyze the contour of velocity magnitude results and contour of

temperature. Using these configurations, air flows across the drying chamber has longer period of time and will allow the system to absorb more thermal energy because turbulence air flow results in extending residence period of air inside the SSDC. The geometry of the system has been designed in Ansys Fluent-geometry module. The geometries and boundary conditions of SSDC and CSDC are shown in Figure 3. Aluminum has been chosen as the plate's material in the simulations because of its higher thermal conductivity. Thinner mesh has been used at the body of drying chamber to gain more accurate findings. The cylindrical shape with funnel and inclined angle air distributor for SSDC with four tray section has been designed and manufactured. In the same manner, above mentioned procedures have been performed for the CSDC without funnel and no distributor attached to bottom of the drying chamber. The drying chamber has a length of 500mm and a diameter of 500mm. The generated mesh for SSDC and CSDC has 4671253 and 2286537 element number are shown in Figure 4. In the analysis of drying chamber, two configurations of drying chamber have been tested.
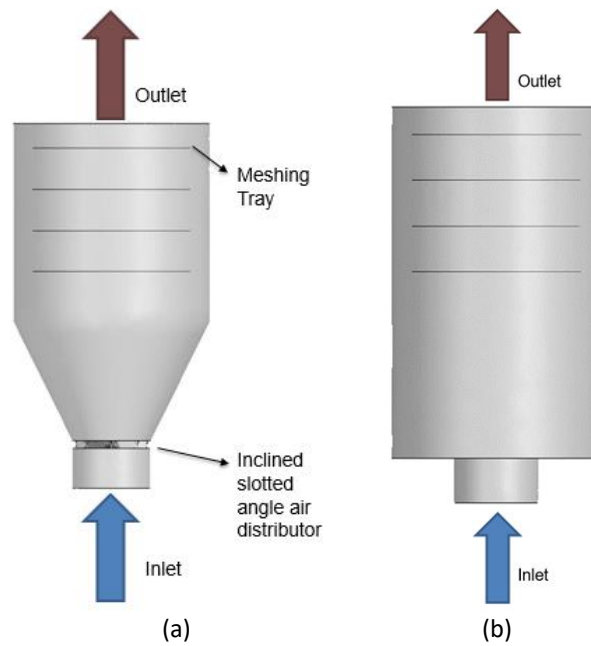
Fig. 3. Boundary condition of solar drying chamber;
(a) SSDC, (b) CSDC
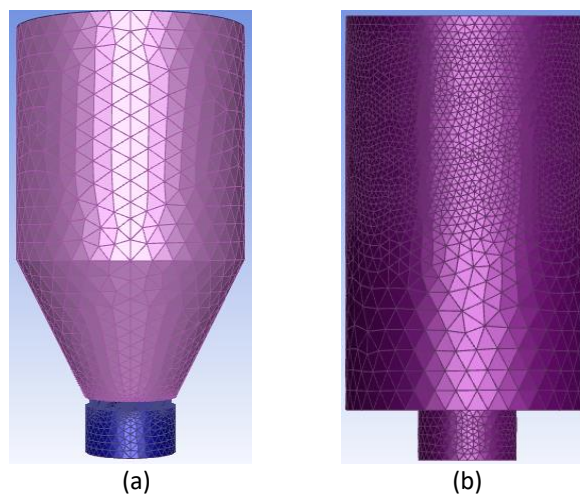
Fig. 4. Generated mesh of solar drying chamber; (a)
SSDC, (b) CSDC

2.2 Experiment Setup

Schematic diagram and setup for solar drying system of a laboratory scale are shown in Figure 5 and Figure 6. The experimental setup consisted of a solar drying chamber with inclined slotted angle air distributor at the air inlet, meshing tray, ventilation fan of 12V and 0.55A, a digital weighing machine, digital thermocouple, a personal computer, a hot wire anemometer to measure inlet air velocity, a power supply system, a control valve, insulator and other support structure. In the experiments, fresh kaffir lime leaves were harvested from local farm, Malaysia. The system was operated in mode 3 as presented in Table 1.

Table 1
Modes in the solar drying system

Mode	Heat source
1	Collector
2	Auxiliary Heater
3	Hybrid (Collector + Auxiliary Heater)

The experiment was carried out with outdoor conditions. The drying chamber was made from stainless steel with diameter of 0.5m and height of 0.5m as depicted in Figure 1. In the C-SDC, an air inlet without distributor plate was set up at the bottom of the chamber where for the S-SDC, the distributor was placed at an inlet by the inclined slotted angle air distributor to generate swirling air flow pattern in the drying chamber. The ventilation fans use at inlet and outlet to blow the airflow into the drying chamber and suction air pressure at outlet of the chamber to allow airflow to a lower air pressure region. The inclined slotted angle air distributor used in the present study are also displayed in Figure 2. They were made of LB PLA filament with thickness of 0.01m, 0.02m diameter and 67.5° inclined slotted angle. The distributor was fabricated by 3D printer about 26 hours to complete one fabrication of distributor plate. In the present experiments, the distributor was installed to create swirling air flow pattern and increase the distribution of temperature in the chamber in addition to increase drying performance. The setup of the C-SDC was the same as S-SDC, except that the inclined angle slotted air distributor was not installed. Three 12V DC with 0.55A ventilation fans were used in the solar drying system located at Collector 2, inlet of mixing chamber and at the outlet of drying chamber to control the air velocity as well as to ensure even distribution of air throughout the system. Besides, fans were used to evacuate humidity released by the products during the drying process. The design detail of the solar drying system is illustrated in Table 2.

Table 2
Design detail of the drying chamber and solar dryer

Number of collectors	2
Meshing tray	Stainless steel
Number of meshing trays	4
Distributor material	LB PLA filament
Distributor dimension	0.01m (thickness), 0.02m (diameter)
Insulation material	Insulfex®
	closed-cell elastomeric nitrile rubber foam
Cover plate material	Polycarbonate
Number of ventilation fan	3
Ventilation fan specifications	12V DC, 0.55A
Drying chamber material	Stainless steel
Drying chamber dimension	0.5m (diameter), 0.5 (height)

Total of fourteen digital thermocouples was used in the experiment to record air temperature in the chamber. The positioning of the thermocouple in the experimental setup is described further in Table 3, and the location of each thermocouple was presented in Figure 5.

Table 3
Position of thermocouple in the drying chamber

Thermocouple	Position
T0	Inlet drying chamber
T1, T2, T3	Meshing tray 1
T4, T5, T6	Meshing tray 2
T7, T8, T9	Meshing tray 3
T10, T11, T12	Meshing tray 4
T13	Outlet drying chamber
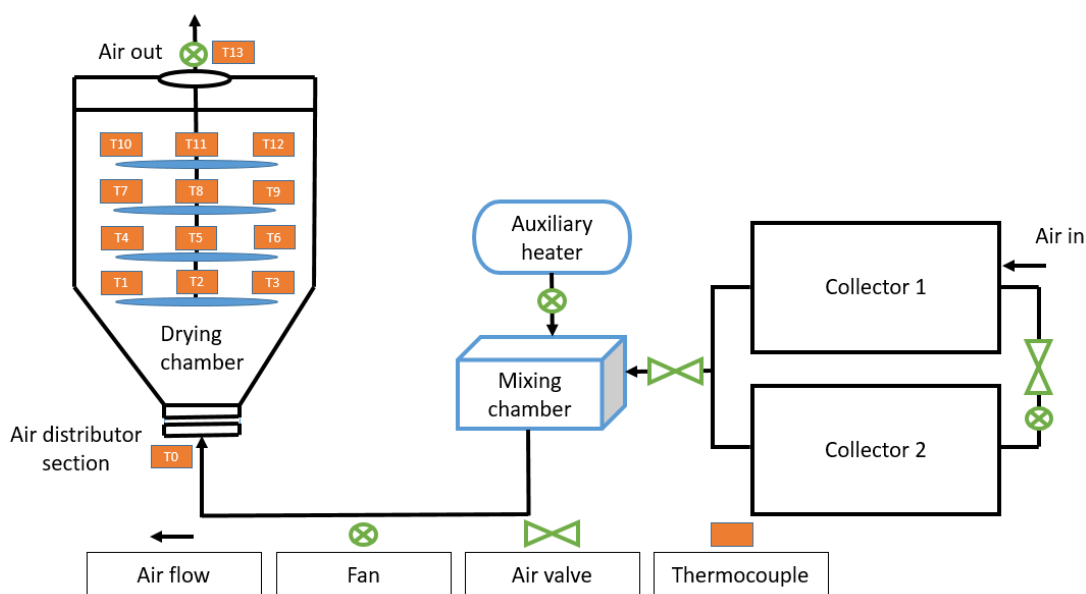
Fig. 5. Schematic diagram of the solar drying system with thermocouple location

During the experiments, inlet bulk air with an average temperature of 50°C, was drawn through two solar collector and a heating section prior to being heated with an electrical heater wrapped along the tube. The electrical heater, rated for 5kW, was used as auxiliary to heat the air entering the chamber. The system was preheated until the apparatus had a constant temperature of 50°C before running the experiment. When the temperature was steady, 260g of fresh kaffir lime leaves were determined by drying the sample at temperature 50°C to 60°C for 7 hours or until the weight became constant and they were loaded into the apparatus. The kaffir lime leaves were sampled every 30min for an hour to determine their moisture content. The volumetric air flow rate was varied to correspond to a velocity of 0.5-2.0m/s. After each drying process, the kaffir lime leaves were removed and digitally weighed and the data recorded to a PC.

Fig. 6. Setup for a solar drying system

2.3 Theoretical Analysis

The power gained in this section was analyzed based on the first law of thermodynamics. The power balance during the experiment was presented in Eq. (1):

$$\dot{Q}_A = \dot{Q}_u + \dot{Q}_{loss} \tag{1}$$

where $\dot{Q}_A$, $\dot{Q}_u$ and $\dot{Q}_{loss}$ were the energy absorbed, useful and loss.

The $\dot{Q}_A$ which the power gained by the collector can be express in Eq. (2) below:

$$\dot{Q}_A = A_c G \tag{2}$$

The power gain in the system involves the mass flow rate of air, the specific heat capacity of the air and also temperature difference between inlet and outlet of the solar collector. The air passing through each collector undergoes convection with the absorber to produce heat that is transferred into the drying chamber. The power balance can be presented by the following equation:

$$\dot{Q}_u = \dot{m}_a C_{pa}(T_o - T_i) \tag{3}$$

The mass flow rate was calculated by measuring the velocity of the air across the collector and using the following expression (4):

$$\dot{m}_a = \rho_a A v_a \tag{4}$$

The power gain is proportional to the temperature difference between the inlet and outlet of the collector. The density of air, ρ_a , assumed to be constant at 1.1 kg/m³, and specific heat capacity of air, C_{pa}, which is 1007 J/kg·K, respectively. Note that Eq. (3) is at a low air temperature range between 40 to 60°C at a pressure of 1 atm.

Drying curves are obtained under controlled conditions provide important information that is related to water transportation mechanisms and they are used to determine the effective diffusion coefficient [17]. The fraction of moisture content (MC) of the kaffir lime leaves at any time of drying process on dry basis of the kaffir lime leaves can be found as:

$$MC = (W_a - W_b)/W_b \qquad (5)$$

Where W_a is the sample initial weight of the kaffir lime leaves at specific time and W_b is the sample dry matter weight (g).

The moisture ratio (MR) is calculated to determine the amount of moisture remaining in the kaffir lime leaves samples reported to the initial moisture content. It can be calculated by using Eq. (6) [18].

$$MR = (M - M_e)/(M_0 - M_e) \qquad (6)$$

Where M_0 is the initial moisture content and M_e is the equilibrium moisture content.

The drying rate (DR) can be expressed as:

$$DR = dM/d_t = (M_{t+dt} - M_{t)})/d_t \qquad (7)$$

Where d_t the time interval dependent derivative and varies depending on the nature of the heat treatment.

The value of Reynolds number is prominent to determine the patterns in a fluid's behavior. The result from the Reynolds number is used to determine whether the fluid flow is laminar or turbulent. The basic formula for Reynolds number is given in Eq. (8):

$$Re = \frac{D_h V}{v_{air}} \qquad (8)$$

The following equation shows the efficiency of the drying chamber:

$$\eta_d = \frac{Pr\, h_{fg}}{(G\, A_c + W)t} \qquad (9)$$

Where Pr the productivity of the system (kg), h_{fg} latent heat of evaporation (J/kg), G the solar irradiance (W/m²), A_c area of collector (m²) and W the auxiliary heater power (W).

2.4 Uncertainty Analysis

The measurements done were subjected to uncertainties, and they were elaborated in this section. The accuracy of each used instrument was determined and presented in Table 4 while the parameters that are studied in this paper involves uncertainty were shown in Table 5 based on the previous study by Moffat [19], Yahya *et al.,* [20] and Sharol *et al.,* [21].

Table 4
Measuring instruments accuracy

Instruments	Quantity	Accuracy
K-type thermocouple	23	−1.5°C to +1.5°C
Pyranometer	1	0.1 W/m^2

Table 5
Parameters uncertainty

Description	Unit	Uncertainty	Relative uncertainty (%)
Outer temperature	°C	±0.10	0.48
Internal temperature	°C	±0.10	0.72
Ambient temperature	°C	±0.10	0.48
Solar radiation	W/m^2	±12	2.04

Every x_n, number of measurements that had been made have the measurement tolerance of σ_n, and the uncertainty of the measurement parameters, U_R, can be calculated by using Eq. (10) [22]:

$$U_R = \left\{ \left(\frac{U_R}{dx_1} . \sigma_1 \right)^2 + \left(\frac{U_R}{dx_2} . \sigma_2 \right)^2 + \left(\frac{U_R}{dx_3} . \sigma_3 \right)^2 + \cdots \left(\frac{U_R}{dx_n} . \sigma_n \right)^2 \right\}^{\frac{1}{2}} \tag{10}$$

Based on the Eq. (6), the uncertainty of the power gained by the system was 314.14±7.68W with relative uncertainty 2.45%.

3. Results and Discussion
3.1 Simulation Result

The numerical simulations using the RNG k-ε turbulent model showed that when the inflow direction of the airflow is inclined through the distributor slots, air flow pattern inside the drying chamber was shown to produce swirling motion in a vicinity of the distributors. Intriguingly, the induced swirling air motion eliminates major dead zone regions. The solar drying chamber has been analyze numerically in order to examine the influences of S-SDC and C-SDC to visualize air flow structure and temperature distribution. Three-dimensional contour of velocity of the flow field is presented in Figure 7, in order to show velocity distribution in the air domain for S-SDC and C-SDC.
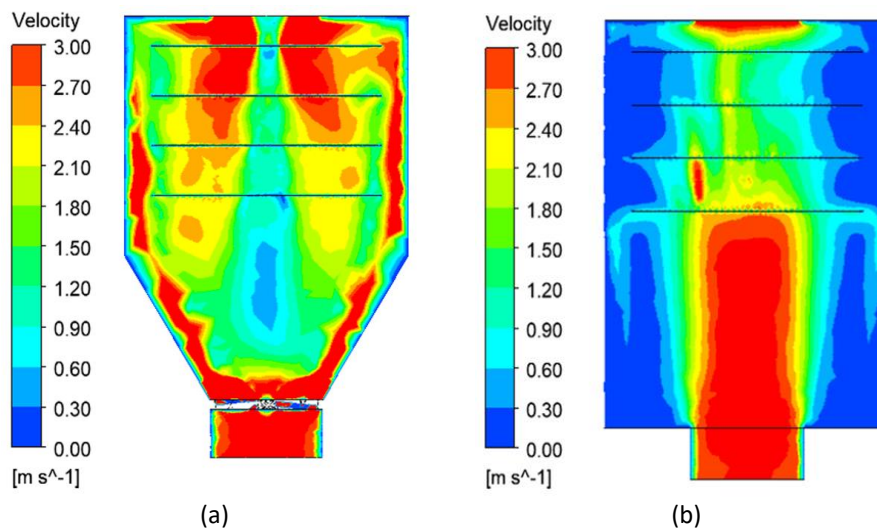
Fig. 7. Contour of velocity contours results for (a) S-SDC and (b) C-SDC

In order to analyze the flow pattern at different locations inside the drying chamber, five horizontal planes (X-Z) were made through the 3-dimensional fluid domain for SSDC and CSDC. The description of flow dynamics drying chamber is discussed by analyzing the velocity contours from different computational fluid domains. It was found that the flow patterns inside the SSDC were swirling air flow. The velocity contour of SSDC in Figure 7 shows that the air velocity was at its peak value around inlet at inclined angle holes and also at the outlet of the drying chamber. Furthermore, the velocity contour patterns from the simulation revealed that SSDC succeeded in increasing the distribution of incoming airflow from the inlet hot air solar absorber. The 'dead zones' as appeared in SSDC seemed less than compared to CSDC. The velocity contours indicated that large dead zones were formed around the side of CSDC caused by laminar air flow pattern across the chamber. This suggests that the type of CSDC air flow was nearly impossible to give uniform air flow in the drying chamber with no distributor applied otherwise low pressured fan blower was replaced with the pressurized air. As can be seen through the velocity contours in Figure 7, the inclined air injection produces swirling air motion in a clock-wise direction. Consequently, a 'sweeping effect' of the air flow as a result from the swirling motion of air through the inclined entry of the slots eliminates a major dead zone region that has been previously observed in the crossed section planes at the bottom of drying chamber. The contours of air velocity in Figure 7 provides an evidence of distinctive swirling motion inside the drying chamber. The swirling intensity for the 67° distributor was high at the distributor region. The investigation of air flow behaviors in the C-SDC and S-SDC was performed at a constant air velocity 3.0 m/s. The flow in the C-SDC did not significantly change with the height of the chamber. In the swirling solar drying chamber (S-SDC), swirling air flow pattern were detected just above the air inlet (near the inclined angle slotted air distributor) which improve air distribution in the chamber thus increase the performance of kaffir lime leaves drying rate. The multiple swirling flows helped promote turbulence air flow which facilitated contact between the kaffir lime leaves and hot air and thus accelerating the removal moisture from the crop.

In the Figure 8, flow field temperature distribution of the drying chamber is displayed from top view. The performance of the distributors was further assessed in terms of temperature distribution using SSDC and CSDC. The distribution of temperature covered in the SSDC is increasing and distributed fairly uniform at inside, top and middle peripheral of the drying chamber compared to CSDC. Non-uniform temperature distribution of the CSDC was detected at the bottom peripheral of the drying chamber operated with no distributor. The case, however, was different in SSDC operated by 67° inclined angle air distributor where the temperature distribution was recorded uniform at the bottom region of the drying chamber. The air flow passes over the chamber and gets a portion of the thermal energy. From the results it can be seen that S-SDC collect a higher percentage of thermal energy in comparison to C-SDC. It can be stated that, using an inclined slotted angle air distributor as medium to change the air flow pattern in the chamber consequently causes to raise the temperature distribution and extending the present time of the air inside S-SDC. The numerical analysis confirms that with turbulence air flow pattern inside chamber give a positive influence on efficiency of S-SDC. Therefore, as it is clear from the results, S-SDC has higher efficiency and better thermal performance in comparison to C-SDC.
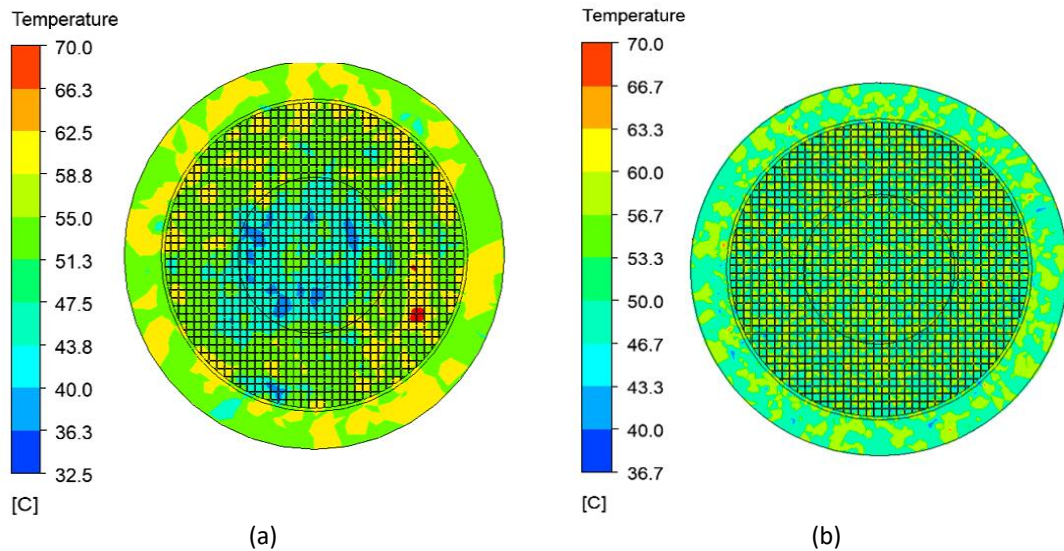
Fig. 8. Contour of temperature in (a) S-SDC and (b) C-SDC

3.2 Experimental Result

The relationship between the moisture content and the drying rate of kaffir lime leaves was presented in Figure 9. From the results, it can be observed that the drying rate of the kaffir lime leaves was higher at the initial stages, where high moisture content was available in the leaves. This is because the heat energy was easily evaporating the moisture at the surface of the leaves from the heated air that passed through each layer of trays. However, as the drying process continued, the drying rate decreased as the moisture content inside the leaves became less. It was because the evaporative zone moved to the inside of the leaves, causing less moisture to evaporate to the surrounding. It also can be seen that the drying rate of the SSDC system was higher at the initial stage, compared to drying rate of CSDC. The heat supplied by SSDC provided high energy to bring down moisture content at a higher rate. Drying rate of SSDC was higher and faster compared to CSDC from 3.03 to 1.73 and 3.07 to 1.77 at highest air velocity. The heated air during the experiment carried lower energy which slowed down the evaporation process.
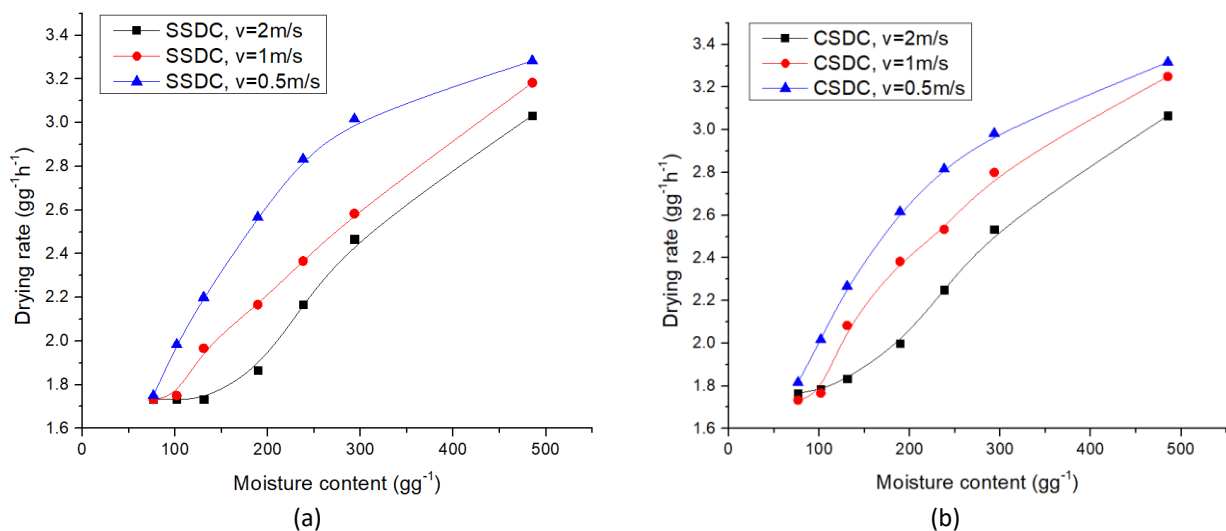
Fig. 9. Relationship between drying rate (DR) and moisture content (MC) for kaffir lime leaves at various air velocity in a (a) (C-SDC) and (b) swirling solar drying chamber (S-SDC) with inclined slotted angle air distributor

The drying curve for all two experiments between SSDC and CSDC were shown in Figure 10. The changes of moisture content of the kaffir lime leaves were measured for every 30 minutes until it reached equilibrium moisture content. From the experiments carried out, it was observed that the fastest drying period of using SSDC took about 4.2 hours while for CSDC took about 5.8 hours. This was due to the fact that the kaffir lime leaves in SSDC received more heat energy, supplied by the auxiliary heater apart from the solar collector which produced heat by the solar radiation from the sun and being transported into the drying chamber by forced convection. Meanwhile, the kaffir lime leaves that being dried CSDC has a good drying period only at the center of the drying chamber. As a result, the drying time of the SSDC was found to be shorter than CSDC. The SSDC take shorter time for drying due to the drying chamber able to provide enough heat energy and distribute optimum air flow rate to support the dryer system which led to constant ideal air temperature during the drying process.
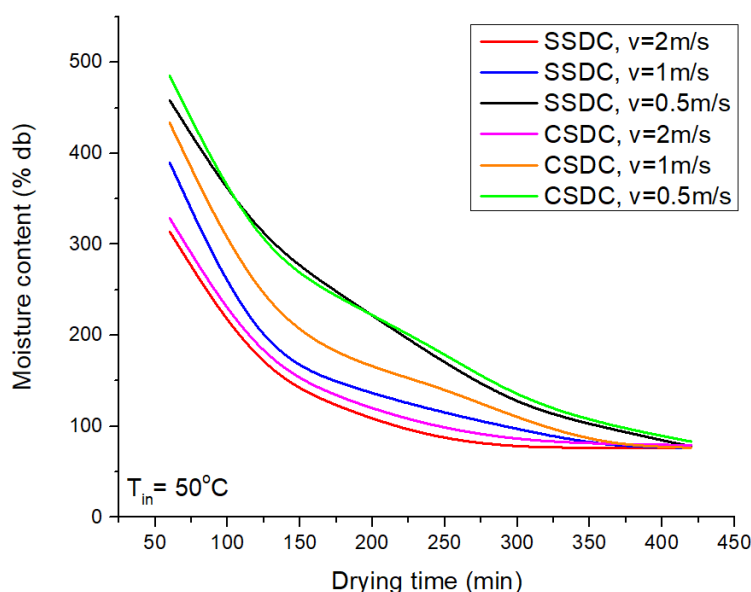
Fig. 10. Relationship between moisture content (MC) and drying time (DT, minutes) for kaffir lime leaves at various air velocity in a conventional solar drying chamber (C-SDC) and swirling solar drying chamber (S-SDC) with inclined slotted angle air distributor

The moisture ratio vs drying time for each layer of trays are shown in Figure 11. From the results, it showed that the air velocity had a significant effect on the drying period of kaffir lime leaves. Higher air velocity produced steeper drying curve which means the increase of the air velocity during the drying activity can reduce the time required to achieve certain moisture content. With high air velocity, the air can carry greater heat energy that was being move in drying chamber from inlet to outlet since lesser chance of heat losses to the surrounding. From the graph, the trend showed that the moisture ratio decreased rapidly at the initial phase. This is due to sufficient water film that presented on the surface of the kaffir lime leaves. So, the moisture is evaporated easily as the water from the inside is being transferred to the surface of the leaves. As the drying process continued, the moisture ratio value against time slowly decreased since only some parts of the surface are still having water film. There is not sufficient water inside the leaves that can be transferred to the surface.
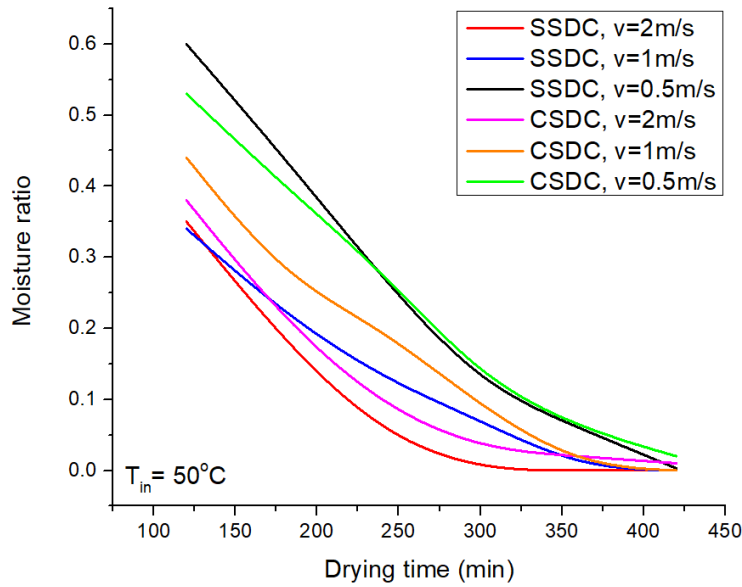
Fig. 11. Relationship between moisture ratio (MR) and drying time (DT, minutes) for kaffir lime leaves at various air velocity in a conventional solar drying chamber (C-SDC) and swirling solar drying chamber (S-SDC) with inclined slotted angle air distributor

Figure 12 presented the comparison of drying rate at different air velocity from SSDC and CSDC. From the results, the leaves at SSDC at velocity of 2m/s dried faster than the others. The heated air is being inhaled from the inlet of drying chamber which is located at the bottom. So, the air with high heat energy initially passed through the kaffir lime leaves located at the bottom tray before it moved upwards. Higher heat is being absorbed by the leaves at SSDC compared CSDC which caused the water evaporated at higher rate.
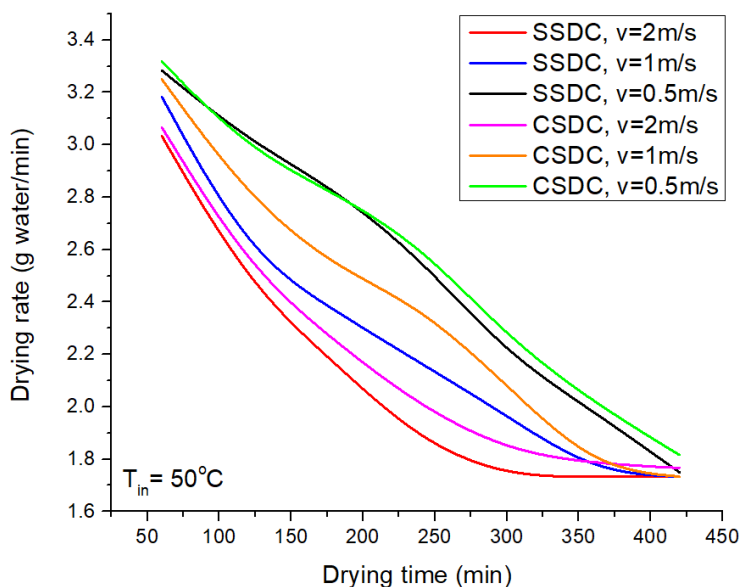
Fig. 12. Relationship between drying rate (DR) and drying time (DT, minutes) for kaffir lime leaves at various air velocity in a conventional solar drying chamber (C-SDC) and swirling solar drying chamber (S-SDC) with inclined slotted angle air distributor

The overall results of the flow and drying characterization in the swirling solar drying chamber (S-SDC) at various air velocities (0.5, 1.0 and 2.0m/s) are reported together with those of typical conventional solar drying chamber (C-SDC). The influences of drying time and air velocity on the moisture content ratio and drying rate are presented in Figure 12 and Figure 13. Generally, the drying rate of kaffir lime leaves abruptly decrease in the first stage of drying process (after 1 hour) and thereafter the moisture content gradually increased. At the same drying time, moisture content decrease with increasing air velocity due to the increased quantity of the moisture carrier (air) and stronger turbulence. Additionally, at low air velocities, the kaffir lime leaves were densely packed leading to inefficient water vaporization. For the S-SDC, the reduction moisture content ratio and drying rate at the highest air velocity (2.0 m/s) were greater than those at (0.5 and 1.5 m/s). At the same drying time and air velocity, the reduction rate of moisture content and drying rate in in the S-SDC was higher than in the C-SDC. This indicates that the evaporation of water and thus moisture removal is enhanced by the swirl effect. Additionally, swirl flow helps in increasing air velocity, since the same throughput must be accommodated by an increase flow mixing, resulting in larger flow and temperature gradients, the effective driving potentials for heat and mass transfer. All air velocities (0.5, 1.5 and 2.0m/s), the drying rates in the (S-SDC) were higher than those in the (C-SDC).
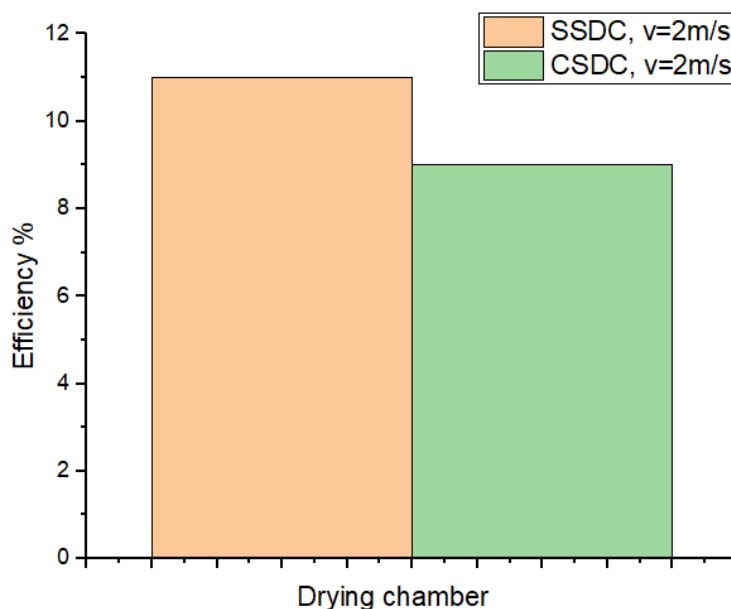
Fig. 13. Drying chamber efficiency of the SSDC and CSDC

Two drying tests of kaffir lime leaves were conducted using SSDC and CSDC collector. The parameter for the drying process is set at 900W/m2 of artificial solar radiation and air velocity of 2.0m/s. A total of 60g of kaffir lime leaves was placed on one layers of trays, and they were dried until they reached their equilibrium mass of 11 g. Figure 11 and Figure 12 show the results of the drying activities. It can be deduced that the drying period using SSDC time taken was 4.1 hours, while for CSDC the time taken was 5.8 hours. This is due to different heated air temperature achieved inside the drying chamber when using both configurations. The average air temperature for the SSDC was 48.5°C while for CSDC it was 46.1°C. The trend shows that drying time is inversely proportional to air temperature. With the increase in air temperature, the time required to reduce the kaffir lime leaves mass decreases. Higher air temperature can lead to higher energy availability to remove moisture from the kaffir lime leaves, hence resulting in a higher drying rate for the process. The efficiency of the system at highest air velocity on one of the trays is calculated, and it shows that the efficiency by using SSDC is 11% whereas lower efficiency is produced by CSDC, which is 9.1% as shown in Figure

13. From the presented results, it can be seen that the increase of drying chamber thermal performance resulting from utilizing the SSDC configuration with optimum the parameters. Improving solar drying system is a crucial step in order to increase the performance and efficiency of a solar dryer. Integrating drying chamber thermal performance is very convenient in drying activity to overcome heat losses during drying, and this will lead to an increase yield and reducing time in solar dryer usage in the agricultural sector.

4. Conclusions

The configuration of SSDC and CSDC affects the performance of a solar drying system. SSDC has higher efficiency compared to CSDC with regards to the moisture content (MC), moisture content ratio (MR) and drying rate (DR) that were examined at air velocities of 0.5, 1.0 and 2.0m/s. The numerical analysis confirms that with swirling air flow pattern inside the drying chamber showed increasing distribution of air flow and temperature covered hence give a positive influence on efficiency of S-SDC. The experimental results showed that the S-SDC fitted with an inclined angle air distributor at the bottom of the chamber reduced the kaffir lime leaves moisture content ratio better than a C-SDC. The S-SDC also has a higher drying rate and decreased drying time as compared to a C-SDC from 3.03 to 1.73 and 3.07 to 1.77. It was also found that drying at higher air velocities results in a greater rate of reduction in the moisture content ratio or drying rate due to increase the quantity of moisture carrier (air) and stronger turbulence. SSDC has higher efficiency compared to CSDC of 11% compared to 9.1% for both configurations.

References

[1] Senthil, R., Gauri Phadtare, and G. Vijayan, "A parametric study on effect of drying performance of solar dryer integrated with a dehumidifier unit." *International Journal of Emerging Trends in Engineering Research* 8, no. 6 (2020): 2321-2326. https://doi.org/10.30534/ijeter/2020/19862020

[2] Daghigh, Roonak, Roonak Shahidian, and Hooman Oramipoor. "A multistate investigation of a solar dryer coupled with photovoltaic thermal collector and evacuated tube collector." *Solar Energy* 199 (2020): 694-703. https://doi.org/10.1016/j.solener.2020.02.069

[3] Rabha, D. K., and P. Muthukumar. "Performance studies on a forced convection solar dryer integrated with a paraffin wax-based latent heat storage system." *Solar Energy* 149 (2017): 214-226. https://doi.org/10.1016/j.solener.2017.04.012

[4] Etim, Promise Joseph, Akachukwu Ben Eke, and Kayode Joshua Simonyan. "Design and development of an active indirect solar dryer for cooking banana." *Scientific African* 8 (2020): e00463. https://doi.org/10.1016/j.sciaf.2020.e00463

[5] Mehta, Pranav, Shilpa Samaddar, Pankaj Patel, Bhupendra Markam, and Subarna Maiti. "Design and performance analysis of a mixed mode tent-type solar dryer for fish-drying in coastal areas." *Solar Energy* 170 (2018): 671-681. https://doi.org/10.1016/j.solener.2018.05.095

[6] Gulcimen, Fevzi, Hakan Karakaya, and Aydın Durmus. "Drying of sweet basil with solar air collectors." *Renewable Energy* 93 (2016): 77-86. https://doi.org/10.1016/j.renene.2016.02.033

[7] Tarminzi, M. A. S. M., A. A. Razak, M. A. A. Azmi, A. Fazlizan, Z. A. A. Majid, and K. Sopian. "Comparative study on thermal performance of cross-matrix absorber solar collector with series and parallel configurations." *Case Studies in Thermal Engineering* 25 (2021): 100935. https://doi.org/10.1016/j.csite.2021.100935

[8] Islam, Majedul, Md Imrul Islam, Mehedi Tusar, and Amir Hamza Limon. "Effect of cover design on moisture removal rate of a cabinet type solar dryer for food drying application." *Energy Procedia* 160 (2019): 769-776. https://doi.org/10.1016/j.egypro.2019.02.181

[9]   Khanchi, A., and S. Birrell. "Drying models to estimate moisture change in switchgrass and corn stover based on weather conditions and swath density." *Agricultural and Forest Meteorology* 237 (2017): 1-8. https://doi.org/10.1016/j.agrformet.2017.01.019

[10]   Çakmak, Gülşah, and Cengiz Yıldız. "Design of a new solar dryer system with swirling flow for drying seeded grape." *International Communications in Heat and Mass Transfer* 36, no. 9 (2009): 984-990. https://doi.org/10.1016/j.icheatmasstransfer.2009.06.012

[11]   Mustayen, A. G. M. B., S. Mekhilef, and R. Saidur. "Performance study of different solar dryers: A review." *Renewable and Sustainable Energy Reviews* 34 (2014): 463-470. https://doi.org/10.1016/j.rser.2014.03.020

[12]   Singh, Pushpendra, Vipin Shrivastava, and Anil Kumar. "Recent developments in greenhouse solar drying: A review." *Renewable and Sustainable Energy Reviews* 82 (2018): 3250-3262. https://doi.org/10.1016/j.rser.2017.10.020

[13]   Fudholi, Ahmad, Kamaruzzaman Sopian, Mohd Hafidz Ruslan, M. A. Alghoul, and Mohamad Yusof Sulaiman. "Review of solar dryers for agricultural and marine products." *Renewable and Sustainable Energy Reviews* 14, no. 1 (2010): 1-30. https://doi.org/10.1016/j.rser.2009.07.032

[14]   Lingayat, Abhay, V. P. Chandramohan, and V. R. K. Raju. "Design, development and performance of indirect type solar dryer for banana drying." *Energy Procedia* 109 (2017): 409-416. https://doi.org/10.1016/j.egypro.2017.03.041

[15]   Yudin, Ahmmad Shukrie Md, Shahrani Anuar, and Ahmed N. Oumer. "Improvement on particulate mixing through inclined slotted swirling distributor in a fluidized bed: An experimental study." *Advanced Powder Technology* 27, no. 5 (2016): 2102-2111. https://doi.org/10.1016/j.apt.2016.07.023

[16]   Lubis, Hamzah. "Renewable Energy of Rice Husk for Reducing Fossil Energy in Indonesia." *Journal of Advanced Research in Applied Sciences and Engineering Technology* 11, no. 1 (2018): 17-22.

[17]   Corrêa, Paulo Cesar, Fernando Mendes Botelho, Gabriel Henrique Horta Oliveira, André Luis Duarte Goneli, Osvaldo Resende, and Sílvia de Carvalho Campos. "Modelagem matemática do processo de secagem de espigas de milho." *Acta Scientiarum. Agronomy* 33, no. 4 (2011): 575-581. https://doi.org/10.4025/actasciagron.v33i4.7079

[18]   Tasirin, S. M., I. Puspasari, A. W. Lun, P. V. Chai, and W. T. Lee. "Drying of kaffir lime leaves in a fluidized bed dryer with inert particles: Kinetics and quality determination." *Industrial Crops and Products* 61 (2014): 193-201. https://doi.org/10.1016/j.indcrop.2014.07.004

[19]   Moffat, R. J. "Contributions to the theory of single-sample uncertainty analysis." *Transactions of the ASME* 104 (1982): 250-258. https://doi.org/10.1115/1.3241818

[20]   Yahya, M., Ahmad Fudholi, and Kamaruzzaman Sopian. "Energy and exergy analyses of solar-assisted fluidized bed drying integrated with biomass furnace." *Renewable Energy* 105 (2017): 22-29. https://doi.org/10.1016/j.renene.2016.12.049

[21]   Sharol, Ahmad Fadzil, Amir Abdul Razak, Zafri Azran Abdul Majid, and Ahmad Fudholi. "Experimental study on performance of square tube absorber with phase change material." *International Journal of Energy Research* 44, no. 2 (2020): 1000-1011. https://doi.org/10.1002/er.4971

[22]   Sharol, A. F., A. A. Razak, Z. A. A. Majid, M. A. A. Azmi, and M. A. S. M. Tarminzi. "Performance of force circulation cross-matrix absorber solar heater integrated with latent heat energy storage material." In *IOP Conference Series: Materials Science and Engineering*, vol. 469, no. 1, p. 012107. IOP Publishing, 2019. https://doi.org/10.1088/1757-899X/469/1/012107